Reaction-Rate Constants in Steady-State Hollow-Cathode Discharges: $Ar + H_2O$ Reactions

W. Lindinger
Institut für Atomphysik der Universität, Innsbruck, A-6020 Austria
(Received 9 June 1972)

The method described in this paper permits the determination of reaction-rate constants for formation and loss of each type of ion through the measurement of the radial distribution of the various ion densities in the steady-state negative glow of a cylindrical hollow cathode. The method is explained with the following example: A discharge is produced in an $Ar + 0.15\%$ H_2O mixture, and a quantitative examination is made of the principal reactions: $Ar + e \xrightarrow{k_1} Ar^+ + 2e$; $Ar^+ + H_2O \xrightarrow{k_2} ArH^+ + OH$; $ArH^+ + H_2O \xrightarrow{k_3} H_3O^+ + Ar$; $H_2O^+ + H_2O \xrightarrow{k_4} H_3O^+ + OH$; $Ar^+ + H_2O \xrightarrow{k_5} H_2O^+ + Ar$; and $H_3O^+ + e \xrightarrow{\alpha} H_2O + H$, the loss reaction. The reaction constants obtained have the following values, all in units of $cm^3\ sec^{-1}$: $k_1 = 1.2 \times 10^{-7}$; $k_2 = 1.3 \times 10^{-9}$; $k_3 = 4.5 \times 10^{-9}$; $k_4 = 1.3 \times 10^{-9}$, and $k_5 = 1.5 \times 10^{-10}$; $\alpha = 1.1 \times 10^{-6}$. The values of k_4 and α are in good agreement with those given by other authors. The remaining values of constants are believed to be new. A rough estimate is also made of the density of the fast dark-space electrons ($E_{kin} \gtrsim 50$ eV) that exist in the negative glow.

I. INTRODUCTION

By far the largest number of reaction-rate constants ever measured for ion-molecule reactions at thermal ion velocities were obtained by the method of flowing afterglow[1,2] and by stationary afterglows.[3,4] Recently, drift-tube techniques have begun to be widely applied to the study of ion-molecule reactions.[5,6] The steady-state plasma, however, has hardly been used for determining reaction constants.

The first quantitative examination of a reaction in the positive column was made by Pahl,[7] who obtained values for the product $k\tau$, where τ is the mean life of Ar′ (Ar′ indicates excited Ar) and k is the reaction constant for the Hornbeck–Molnar process

$$Ar' + Ar \xrightarrow{k} Ar_2^+ + e\ .$$

Later Gaur and Chanin[8] obtained absolute values of rate constants as a function of the characteristics of the positive column.

Most recently, examinations were made in this laboratory on the ion formation and conversion in the negative glow of a cylindrical hollow cathode,[9,10] and a reaction scheme was set up for Ar with a little water contamination. The relative proportions of the individual ion species were shown to vary considerably with the radial location in the negative glow from which the ions were extracted. This fact forms the basis of the method of determining reaction constants in the active steady-state plasma of a hollow cathode described in this paper.

II. APPARATUS

The apparatus used for the present studies is a modified version of the system described previously.[9,10] A schematic diagram of the equipment is shown in Fig. 1. It consists of a cylindrical hollow cathode of electrolytic copper (diameter 2 cm), with ions being extracted in the axial direction from the negative glow (NG) by means of a sampling probe P (diameter, 1 mm; sampling orifice SO, 50 μm in diameter; molybdenum) at the end of the hollow cathode opposite to the anode A. The ion beam is analyzed by a magnetic 60° mass spectrometer. The cathode and hence also the entire NG can be displaced radially with respect to the sampling probe (see Fig. 1). It is thus possible to extract ions from regions at various distances from the central axis of the NG and thus to determine radial density profiles of individual ion species. A more detailed description is in preparation for publication elsewhere.[11]

III. THEORY

The NG within our hollow cathode is a cylindrical plasma having a radius r_0 (glow edge) that depends considerably on the discharge current I_e and pressure p.[12] The field strength within the plasma is very low if not actually zero. While the density ratios of different ion species in other types of discharges, e.g., in a positive column, are assumed to be constant over the discharge radius r, in the negative glow of the hollow cathode, the density ratio varies considerably with r.[9,10] Within r_0, the steady-state condition for the density of any ionic species X^+ is given by

$$\frac{d[X^+]}{dt} = 0 = D_a \Delta[X^+] + \nu_p - \nu_l - \alpha[X^+][e_s]\ . \qquad (1)$$

Equation (1) holds at any point. Densities are denoted by expressions in brackets. A diffusion term $D_a \Delta[X^+]$ is non-negligible because a strong density gradient exists, causing a significant dif-

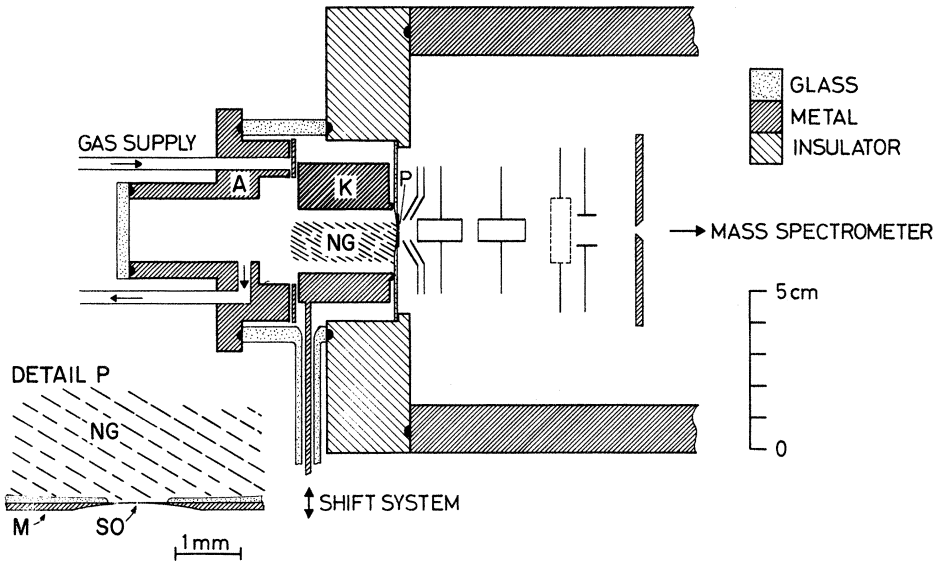

FIG. 1. Schematic drawing of the experimental apparatus. A: anode; K: cathode (2 cm in diameter); NG: negative glow; P: sampling probe; SO: sampling orifice; M: molybdenum.

fusive flow. D_a is the coefficient of ambipolar diffusion; the radial component of $\Delta[X^+]$, in cylindrical coordinates, reads

$$\Delta[X^+]=\frac{\partial^2[X^+]}{\partial r^2}+\frac{1}{r}\frac{\partial[X^+]}{\partial r} .$$

The production of X^+ is described by the term ν_p which is the product of a formation constant k_a and the densities of the reaction partners leading to X^+ production, or the sum of such products in the case of parallel reactions. Losses are due to ion-molecule reactions (IMR), $\nu_l = k_b[X^+][Y]$, including charge exchange, as well as to volume recombination $\alpha[X^+][e_s]$. α is the volume recombination coefficient; $[e_s]$ denotes the density of plasma electrons.

If the steady-state condition (1) set up for a given carrier species X^+ contains n unknown quantities, k_i ($i=1, 2, \ldots, n-1$) and α, where the k_i's are all for one reaction, e.g., k_a or k_b, a total of n linearly independent equations will be required to determine all the values of k_i and α. These n equations are obtained by determining by experiment the values of $D_a\Delta[X^+]$ and the densities of the reaction partners occurring in (1) at n distances r from the glow axis ($r<r_0$). The setting up and solving of these equations for the various ion species are described in Secs. IV and V.

IV. RESULTS OBTAINED FROM AN Ar+0.15% H_2O MIXTURE

Former examinations have shown[9,10] that the main ions that occur in an argon discharge with traces of H_2O are the following: Ar^+, Ar^{++}, Ar_2^+, ArH^+, H_2O^+, and H_3O^+. These are produced (and destroyed) in the negative glow by the following processes:

(a) $Ar^+ : Ar + e_f \xrightarrow{k_1} Ar^+ + 2e$,

(b) $Ar^{++} : Ar + e_f \rightarrow Ar^{++} + 3e$,

electron impact (here e_f means "fast electrons," i.e., fast enough to ionize Ar);

(c) $Ar_2^+ : Ar' + Ar \rightarrow Ar_2^+ + e$,

Hornbeck–Molnar process;

(d) $ArH^+ : Ar^+ + H_2O \xrightarrow{k_2} ArH^+ + OH$,

(e) $H_3O^+ : ArH^+ + H_2O \xrightarrow{k_3} H_3O^+ + Ar$,

(e′) $H_3O^+ : H_2O^+ + H_2O \xrightarrow{k_4} H_3O^+ + OH$,

ion-molecule reactions (IMR);

(f) $H_2O^+ : Ar^+ + H_2O \xrightarrow{k_5} H_2O^+ + Ar$,

charge exchange;

(g) $H_3O^+ + e_s \xrightarrow{\alpha} H_2O + H$,

volume recombination.

H_2O^+ is formed mainly by IMR (secondary process) and not by electron impact (primary process). This is disclosed by the fact that a contribution of H_2O^+ to the total ion density is always several orders of magnitude higher than that of the neutral H_2O contribution to the total neutral density. Later on it will be shown quantitatively that H_2O^+ is produced mainly by process (f). In Ref. 10 this statement could not be made with certainty.

At a discharge pressure of 0.34 torr (Ar with 0.15% H_2O) and a discharge current $I_e=3$ mA, the densities of the different ion species along the axis show the relative percentages listed in Table I. The temperature of the neutral gas and of the ions is assumed to be about 300 °K. The remaining 0.74% consists of traces of H^+, H_2^+, H_3^+, Ar^{++}, N^+, NH^+, O^+, OH^+, N_2^+, N_2H^+, NO^+, $H^+(H_2O)_2$,

TABLE I. Relative densities of ion types.

Ion species	Percentage of the total ion density on the axis
Ar^+	30.83
Ar^{++}	2.17
Ar_2^+	1.56
ArH^+	10.73
H_2O^+	4.67
H_3O^+	49.30
	total 99.26%

CO_2^+, and Cu^+ and of the masses 31, 32, and 68 (ArN_2^+?).

The radial dependence of the ion densities of Ar^+, ArH^+, H_2O^+, and H_3O^+ and of the sum of all ions $\sum X_i^+$ in the negative glow is shown in Fig. 2. The total density $\sum X_i^+$ is equal to the electron density $[e_s]$ because of the quasineutrality of the plasma.

The steady-state condition (1) is used for setting up a density balance of the various ion species. Formation of Ar^+ by reaction (a) is due almost exclusively to the collision of fast electrons $[e_f](E_{kin} \gtrsim 50$ eV) from the dark space with Ar atoms. The cathode fall of potential throughout these measurements was ~300 V. This fast-electron density $[e_f]$ is several orders of magnitude smaller than the density of slow plasma electrons $[e_s]$.[10] At present, the carrier balance of Ar^+ will not be discussed, because up to now it has not been possible to measure directly either the radial dependence of the density of fast dark-space electrons, or the function governing Ar^+ production.

ArH^+

Allowing for the processes (d) and (e),[9,10] the steady-state condition for ArH^+ reads as follows:

$$\frac{d[ArH^+]}{dt} = 0 = D_a \Delta[ArH^+] + k_2[Ar^+][H_2O] - k_3[ArH^+][H_2O] \,. \quad (2)$$

The ratio of $k_2 : k_3$ can be calculated immediately, if $D_a\Delta[ArH^+]$ and the densities $[Ar^+]$, $[ArH^+]$, and $[H_2O]$ are known at one point of the negative glow. If Eq. (2) is satisfied for two different radii r_1 and r_2, it is possible to calculate from repeated use of Eq. (2) the absolute values of k_2 and k_3. The values of $[Ar^+]$ and $[ArH^+]$ at different radii $r < r_0$ are taken from the curves of Fig. 2. $[H_2O]$ is approximately 1.5×10^{13} cm^{-3}. For determining the diffusion term $D_a\Delta[ArH^+]$, the first and the second derivatives of $[ArH^+]$ are found graphically. D_a is calculated from known values of the ion mobility[13–15] μ and T_e. The same mobility value $\mu = 1.7$ cm^2/V sec (at 760 torr) is used for all ions, as the values of μ for any given ion, given by various authors, differ by amounts that are larger than the differences between the μ values of the different ion species. Measurements by Howorka and Pahl[12] yield T_e values ranging from 0.07 to 0.1 eV. At a discharge pressure of 0.34 torr, $D_a = 400$ cm^2/sec.

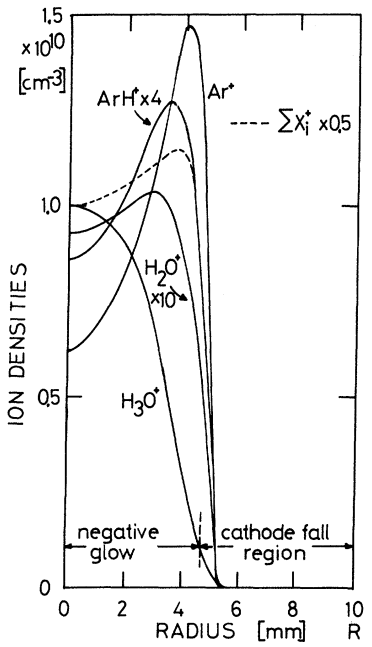

FIG. 2. Radial density profiles for the following ions: Ar^+, ArH^+, H_2O^+, and H_3O^+, and of the sum of all ions $\sum X_i^+$ at a pressure of $p = 0.34$ torr and a discharge current $I_e = 3$ mA.

The values of k_2 and k_3 calculated using four different pairs of r_1 and r_2 are listed in Table II. The difference between the destruction and formation rates of ArH^+,

$$\nu_l - \nu_p = k_3[ArH^+][H_2O] - k_2[Ar^+][H_2O] \,,$$

is calculated for the region $0.5 < r < 3.5$ mm, by using the mean values $\langle k_2 \rangle$ and $\langle k_3 \rangle$ of Table II. The results at various r values are then compared with the values of $D_a\Delta[ArH^+]$. The comparison, shown in Fig. 3, shows good agreement over the

TABLE II. Values of k_2 and k_3 calculated from (2) at different pairs of radii r_1, r_2. Mean values are $\langle k_2 \rangle = 1.31 \times 10^{-9}$ cm^3 sec^{-1}, $\langle k_3 \rangle = 4.51 \times 10^{-9}$ cm^3 sec^{-1}.

r_1 (mm)	r_2 (mm)	k_2 (10^{-9} cm^3 sec^{-1})	k_3 (10^{-9} cm^3 sec^{-1})
0.5	3.5	1.39	4.59
1.0	3.0	1.14	3.94
1.0	2.5	1.10	3.84
2.5	3.5	1.61	5.67

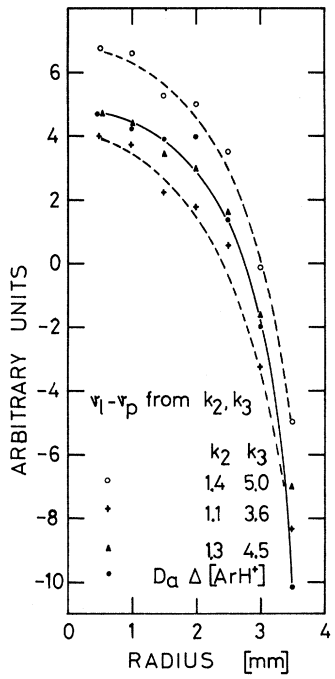

FIG. 3. Comparison of the values of $D_a\Delta[ArH^+]$ obtained from the first and second derivative of the radial variation of $[ArH^+]$ (solid dots) with the radial profiles $\nu_i - \nu_p = k_3[ArH^+][H_2O] - k_2[Ar^+][H_2O]$ calculated with three different pairs of values k_2, and k_3 (in units of 10^{-9} cm^3 sec^{-1}). The figure shows both how well Eq. (2) is satisfied using the best values of k_2 and k_3, and in addition, how strongly a deviation of the k values of about 20% from the best values destroys the agreement. (The curves are drawn as the best fits through the various sets of points.)

entire range of $0.5 < r < 3.5$ mm. In order to demonstrate the accuracy of this method of determining reaction constants, two more sets of points of $\nu_i - \nu_p$ are plotted in Fig. 3 which were calculated using assumed values of k_2 and k_3 that differ by about ± 20% from $\langle k_2 \rangle$ and $\langle k_3 \rangle$. Considerable differences are then found between the diffusion term and $\nu_i - \nu_p$. Since, however, a possible error of up to 40% must be assumed for $[H_2O]$ and a maximum error of 50% for D_a, because of the uncertainty in T_e and μ, the values found for k_2 and k_3 are taken to be correct only to within a factor of 2. This holds also for the results described below.

H_3O^+

H_3O^+ is produced by the processes (e) and (e′) that take place in parallel. As the observed density of $H^+(H_2O)_2$, formed by $H_3O^+ + H_2O \rightarrow H^+(H_2O)_2$,[16] is negligibly small under our experimental conditions, only the volume recombination need be considered as a loss process. The steady-state condition then reads as follows:

$$\frac{d[H_3O^+]}{dt} = 0 = D_a\Delta[H_3O^+] + k_3[ArH^+][H_2O] + k_4[H_2O^+][H_2O] - \alpha[H_3O^+][e_s] , \quad (3)$$

where α is the ion-electron recombination coefficient (as mentioned above). An evaluation of the measured results in analogy to ArH^+ yields the following values *calculated from the* H_3O^+ *balance only*: $k_3 = 4.7\times10^{-9}$ $cm^3 sec^{-1}$, $k_4 = 1.3\times10^{-9}$ $cm^3 sec^{-1}$, and $\alpha = 5.5\times10^{-7}$ $cm^3 sec^{-1}$. Hence, k_3 is in good agreement with the value of $k_3 = 4.5 \times10^{-9}$ $cm^3 sec^{-1}$ obtained from the ArH^+ balance. The process (e′) has been examined quantitatively several times by other authors. The resulting values (Table III) are well supported by the results of the present paper.

For the volume recombination coefficient of H_3O^+, a value of $\alpha = 1.1 \pm 0.2\times10^{-6}$ $cm^3 sec^{-1}$ (at 300 °K) and an assumed temperature dependence $\alpha \sim T_e^{-0.5}$ were given by Biondi *et al.*[20] Our value of α which holds for an electron temperature $T_e \sim 0.1$ eV may be reduced to 300 °K, yielding $\alpha = 1.1\times10^{-6}$ $cm^3 sec^{-1}$ in agreement with Biondi's value.

H_2O^+

Process (e′) is probably the only decisive loss reaction for H_2O^+. The question how far reaction (f) is alone responsible for production of H_2O^+ may be checked by means of the steady-state condition for H_2O^+:

$$\frac{d[H_2O^+]}{dt} = 0 = D_a\Delta[H_2O^+] + k'[X][Y] - k_4[H_2O^+][H_2O] . \quad (4)$$

Using the reaction constant k_4 determined above and the value $D_a\Delta[H_2O^+]$ obtained from the measured results, as well as the densities $[H_2O^+]$ and $[H_2O]$, all terms of Eq. (4) are fixed, except for $\nu_p' = k'[X][Y]$, the production function of H_2O^+, in which k', X, and Y are to be identified. The radial dependence of ν_p' can be calculated by means of (4). As Fig. 4 shows, the curve of ν_p' as a function of r has nearly the same shape as that of $[Ar^+]$. It may therefore be assumed that H_2O^+ is formed according to (f), i.e., mainly by charge exchange of Ar^+ and H_2O. Therefore, $k'[X][Y]$

TABLE III. Values for the reaction-rate constant of the process $H_3O^+ + H_2O \xrightarrow{k_4} H_3O^+ + OH$.

Ref.	$k_4(10^{-9}$ cm^3 $sec^{-1})$	
Hasted (Ref. 17) (value of Talrose *et al.*)	0.85	(410 °K)
Good *et al.* (Ref. 18)	1.8	(300 °K)
Gupta *et al.* (Ref. 19)	1.6	
this work	1.3	(300 °K)

very probably equals $k_5[Ar^+][H_2O]$. The resulting reaction constant k_5 is 1.5×10^{-10} cm^3 sec^{-1}, a value which lies in a range typical of charge-exchange processes.[2] The sum of k_2+k_5 was found by Howard *et al.*[21] to be $(1.43\pm0.1)\times10^{-9}$ cm^3 sec^{-1}, which is in good agreement with the sum of the values found here. The agreement in fact suggests that the values of all the k's may be better than the factor of 2 suggested above.

Ar^+

The results described so far make it possible to set up the steady-state condition (5) for Ar^+. For the production of Ar^+, process (a) is considered; for the loss of Ar^+, the reactions (d) and (f). (A rough estimate shows that the production of Ar^+ by charge exchange between Ar^{++} and Ar may be neglected.)

$$\frac{d[Ar^+]}{dt} = D_a\Delta[Ar^+] + k_1[e_f][Ar] - k_2[Ar^+][H_2O] - k_5[Ar^+][H_2O] \ . \quad (5)$$

All the quantities are known except for k_1 and $[e_f]$, i.e., the density of fast electrons ($\gtrsim 50$ eV, see above). The function $k_1[e_f][Ar]$ and, therefore, the product $k_1[e_f]$ are determined from (5) as described for H_2O^+ production. The reaction constants $k_2=1.3\times10^{-9}$ and $k_5=1.5\times10^{-10}$ from above are used. The radial dependence of the product $k_1[e_f]$ calculated for $I_e=3$ mA and $p=0.34$ torr from (5) is shown in Fig. 5.

A standard relationship between the reaction-rate constant k and the collision cross section σ for a two-body reaction is

$$k=\langle\sigma v\rangle \ ,$$

where v is the collision velocity and the averaging process is carried out over the distribution of velocities. In the case of the formation of Ar^+, we have chosen to define k_1 with the specification that the averaging process is only to be carried out over those electron velocities that are large enough that ionization is possible. The symbol $[e_f]$ refers to the density of such "fast" electrons. The value of σ_i for Ar as a function of electron velocity (or kinetic energy) is well known[22]; it is the hump-shaped curve that starts from zero at a velocity corresponding to the 15.7-eV ionization potential of Ar, reaches a peak value at 50–75 eV, and tails off slowly at higher velocities or energies. For approximate calculations, the value of $\langle\sigma v\rangle$ may be replaced by $\langle\sigma\rangle\langle v\rangle$, in which we put $\langle\sigma\rangle\sim2\times10^{-16}$ cm^2 and $\langle v\rangle\sim6\times10^8$ cm/sec (100 eV). Then $\langle\sigma\rangle\langle v\rangle$ or k_1 emerges as approximately 1.2×10^{-7} cm^3 sec^{-1}.

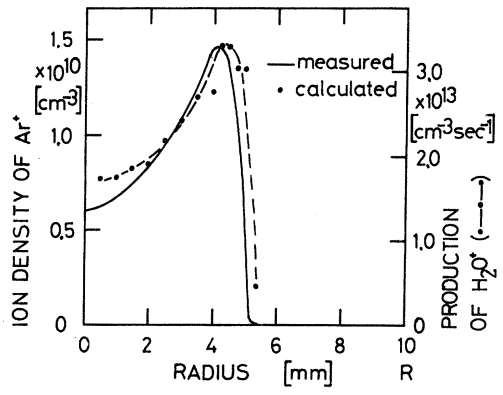

FIG. 4. Comparison of the measured density $[Ar^+]$ and the calculated product $k_5[Ar^+][H_2O]$, which gives the production of H_2O^+ in Eq. (4) (dashed curve). The similarity of the curves is used to establish that H_2O^+ is produced by reaction (f).

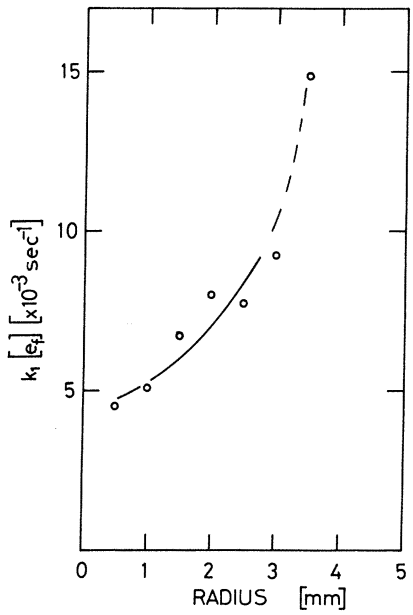

FIG. 5. Radial profiles of the product $k_1[e_f]$.

In Fig. 5, the experimentally measured product $k_1[e_f]$ is shown as a function of the radial position in the hollow cathode. Taking an average value of this quantity as 10×10^{-3} and using k_1 above, the value of $[e_f]$ becomes 8.3×10^4 fast electrons/cm^3. It should be noted that none of the quantities k_1, $[e_f]$ or the product $k_1[e_f]$ are constants, and it is especially important not to conclude from these averaging procedures that $[e_f]$ is constant across the plasma.

The density of dark-space electrons in the negative glow may be estimated also from measurements of the electronic current i_e coming through the sampling orifice with a strongly negative sampling-probe potential[9,10] (~100 V negative with

respect to the plasma potential). An electron density of $[e_f] \sim 1 \times 10^5$ cm^{-3} is found for similar discharge conditions, with $i_e = \frac{1}{4}[e_f]e\bar{v}F$ [$\bar{v}$ is the mean velocity of fast electrons (~100 eV), F is the area of sampling orifice]. The fast-electron density measured in this way agrees well with the density obtained by the first method [steady-state condition (5) for production of Ar^+].

V. CONCLUSION

The described method of determining reaction constants is easy to apply especially for reactions between a principal ion species and a low admixture of a neutral gas or impurity in the discharge gas. In many cases [cf. Eq. (2)], the reaction constants may be determined knowing only relative densities of the individual ion species. The absolute values of densities along the radius, however, must be known for examining primary processes [Eq. (1)] quantitatively, and for examining volume recombination processes [Eq. (3)]. The special advantage of the method lies in the fact that the radial density profiles need only to be determined at one pressure and one discharge current intensity, and that almost every reaction constant can be obtained by two different routes. This also establishes the accuracy of the assumed reactions to a higher degree of certainty. A further advantage lies in the characteristic of the hollow-cathode discharge that the processes all occur under steady-state conditions in a field-free region. Finally, because of the high degree of stability of the plasma in the hollow cathode, the results are highly reproducible.

Measurements have also been made at other pressures and discharge currents. The results agree closely with those given above.

ACKNOWLEDGMENTS

The author wishes to express his thanks to Dr. M. Pahl under whose direction the work was undertaken, to Dr. F. Howorka who assisted extensively in the work of the project, and to Dr. R. N. Varney, Fulbright Professor of Atomic Physics at Innsbruck, for many helpful consultations which led to the successful analysis of the observations, and for assistance with preparation of the manuscript.

[1]F. C. Fehsenfeld, A. L. Schmeltekopf, P. D. Goldan, H. J. Schiff, and E. E. Ferguson, J. Chem. Phys. 44, 4087 (1966).

[2]F. C. Fehsenfeld, A. L. Schmeltekopf, D. B. Dunkin, and E. E. Ferguson, U. S. Commerce Dept. ESSA Technical Report No. ERL 135-Al 3, Boulder, Colorado, 1969 (unpublished).

[3]A. V. Phelps and S. C. Brown, Phys. Rev. 86, 102 (1952).

[4]T. D. Märk and H. J. Oskam, Phys. Rev. A 4, 1445 (1971); Z. Physik 247, 84 (1971); Acta Phys. Austriaca 35, 214 (1972).

[5]E. W. McDaniel and M. R. C. McDowell, *Case Studies in Atomic Collision Physics* (North-Holland, Amsterdam, 1969), Chap. 1.

[6]R. N. Varney, Phys. Rev. 174, 165 (1968).

[7]M. Pahl, Z. Naturforsch. 13a, 753 (1958); 18a, 1276 (1963).

[8]J. P. Gaur and L. M. Chanin, Phys. Rev. 182, 167 (1969).

[9]W. Lindinger, thesis (Universität Innsbruck, Austria, 1971) (unpublished).

[10]M. Pahl, W. Lindinger, and F. Howorka, Z. Naturforsch. 27a, 678 (1972).

[11]F. Howorka, W. Lindinger, and M. Pahl (unpublished).

[12]F. Howorka and M. Pahl, Z. Naturforsch. (to be published).

[13]K. B. McAfee, Jr., D. Sipler, and D. Edelson, Phys. Rev. 160, 130 (1967).

[14]L. B. Loeb, *Basic Processes of Gaseous Electronics* (California U. P., Berkeley, 1961), p. 91ff.

[15]J. A. Hornbeck, Phys. Rev. 83, 374; 84, 615 (1951).

[16]P. F. Knewstubb and A. W. Tickner, in Proceedings of the Eighth Annual Meeting of the American Society for Testing Materials Committee E14 on Mass Spectrometry, Atlantic City, 1960 (unpublished).

[17]J. B. Hasted, *Physics of Atomic Collisions* (Butterworths, London, 1964), p. 489.

[18]A. Good, D. A. Durden, and P. Kebarle, J. Chem. Phys. 52, 212 (1970).

[19]S. K. Gupta, E. G. Jones, A. G. Harrison, and J. J. Myher, Can. J. Chem. 45, 3107 (1967).

[20]M. A. Biondi, M. P. Leu, and A. Johnsen, in Proceedings of Committee on Space Research Symposium on *D* and *E* Region Ion Chemistry, Urbana, Illinois, 1971 (unpublished).

[21]C. J. Howard, H. W. Rundle, and F. Kaufmann, J. Chem. Phys. 53, 3745 (1970).

[22]S. C. Brown, *Basic Data of Plasma Physics* (Wiley, New York, 1959), p. 111; see also Ref. 17, p. 230.